



Acute Myocardial Infarction and Postinfarction Remodeling

10

Christopher M. Kramer and Michael Salerno

Introduction

Cardiac magnetic resonance (CMR) is ideally suited to evaluate the consequences of myocardial ischemia and infarction (MI) because of its excellent spatial resolution and ability to characterize tissue. With the advent of surface coils and segmented k-space cine imaging in the early 1990s enabling imaging in a breath-hold, CMR became practical in patients with acute coronary syndromes (ACS) including MI. Initial studies in acute MI involved imaging of myocardial function, infarct artery patency, and first-pass myocardial perfusion imaging [1]. It was noted that in some infarcts, areas of microvascular obstruction could be visualized which denoted worse outcome for those patients [2]. At the turn of the millennium, the development of an inversion recovery gradient echo pulse sequence [3] allowed excellent nulling of normal myocardial signal, and thus late gadolinium enhancement became a gold standard method of imaging and sizing of infarction and assessing viability [4]. After 2005 or so, T2-weighted (W) imaging of myocardial edema came to the fore as a means to assess the area at risk [5]. T2*-W imaging was later noted to optimally delineate intramyocardial hemorrhage [6]. More lately, T1- and T2-mapping techniques have begun to replace qualitative imaging of infarct size and area at risk [7]. Many of these findings can aid in the prediction of subsequent LV dilation and dysfunction, termed LV remodeling. CMR can identify post-MI complications including myocardial rupture, ventricular septal defects, papillary muscle rupture, and pericarditis. Putting all of these techniques together has advanced the field and has allowed CMR to develop into a comprehensive imaging method for assessing the myocardium in the patient with acute MI.

C. M. Kramer (✉)
Departments of Radiology and Medicine, University of Virginia Health System, Charlottesville, VA, USA
e-mail: ckramer@virginia.edu

M. Salerno
Departments of Medicine, Radiology, and Biomedical Engineering, University of Virginia Health System, Charlottesville, VA, USA

Guideline Indication for CMR in Acute MI

A recent consensus statement examined the role of CMR in a number of cardiac conditions including acute MI [8]. This document reviewed the use of LGE, the identification of MO, and the identification of border zones around the acute infarct. The ACC/AHA 2005 Guideline Update for heart failure identified the use of LGE to identify myocardial scar and assess viability [9]. The Appropriateness Criteria for CMR identified the appropriate use of CMR for assessing patients post-MI including scar and MO and to assess the likelihood of recovery of function with revascularization [10]. Multimodality Appropriate Use Criteria are presently in development to identify the appropriate use of imaging modalities including CMR in acute coronary syndromes and after acute MI. As the use of CMR continues to expand, it is quite likely future guidelines will identify additional appropriate uses of this versatile technology.

CMR Techniques Used in Acute MI

Cine Imaging: LV Structure and Function

In the wake of an acute myocardial infarction (AMI), accurate assessment of the left ventricle (LV) is of paramount importance as functional impairment and/or chamber dilation predicts increased mortality. In a study of 866 post-infarct patients, a resting LV ejection fraction (EF) <40% predicted higher 1-year mortality than did an LVEF >40% [11]. Although LVEF is a powerful predictor of post-infarct survival, end-systolic volume (ESV) is superior as a prognostic parameter. This was demonstrated by White et al. who enrolled 605 patients following AMI and followed them for an average of 78 months. Ultimately, ESV was the best predictor of survival, and neither LVEF nor end-diastolic volume (EDV) added prognostic value [12].

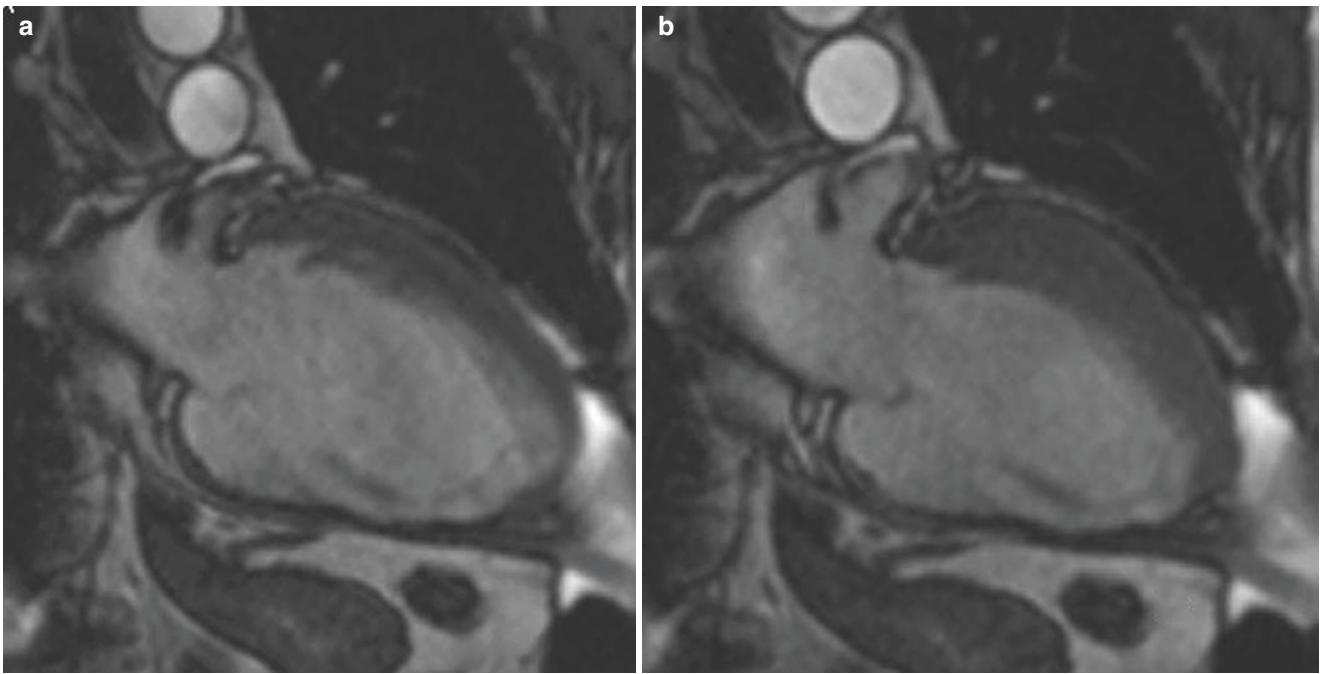


Fig. 10.1 (a) End-diastolic 2-chamber long-axis SSFP image in a patient with a chronic inferior wall MI with wall thinning. (b) End-systolic image from the same series demonstrating normal thickening of the anterior wall and akinesis of the inferior wall

Steady-state free precession cine CMR covering the LV short axis from apex to base allows generation of a complete three-dimensional data set with high temporal and spatial resolution (Fig. 10.1). Measurements made with this data set do not require geometric assumptions and are therefore less prone to error than 2D methods such as 2D echocardiography, particularly in ventricles deformed by MI. Furthermore, the large field of view and excellent contrast generated between the myocardium and blood pool facilitates accurate assessment of chamber dimensions and both regional and global function [13]. Interstudy and interscan reproducibility is high, allowing for reduced sample sizes in clinical trials examining interventions in post-MI patients [14, 15].

Techniques such as myocardial tissue tagging [16] or cine displacement-encoded stimulated echo imaging [17] allow more detailed analysis of regional myocardial motion and deformation than cine imaging. Such techniques have demonstrated dysfunction adjacent to [18] and remote from [19] the infarct zone early post-MI that gradually improves over time [18, 20]. Studies have used tagging to demonstrate persistent diastolic dysfunction in regions that have recovered systolic function after reperfused MI [21].

Late Gadolinium Enhancement

Histopathologic studies of AMI have consistently revealed the complex, heterogeneous, and *dynamic* character of infarct zones [22]. This heterogeneity is a consequence of

many factors including the presence and opening of collaterals during and after injury, magnitude of the ischemic insult, and impact of therapeutic interventions [23]. Furthermore, it has been demonstrated that infarcts evolve over time, generally passing through an early, necrotic phase followed by both a fibrotic and remodeling phase that is dominated by the laying down of new collagen and infarct involution [24, 25]. In fact, infarct scar remains biologically active long after ischemic injury, populated by cells involved in collagen turnover and scar tissue contraction, and may therefore never truly reach a “stable” configuration [22].

Late gadolinium enhancement (LGE) refers to regions of scar, necrosis, and/or inflammation discriminated from normal tissue by prolonged retention of gadolinium-based contrast agents (Fig. 10.2). Since the mid-1980s, investigators have appreciated T1 shortening (increased enhancement) in regions of infarction following gadolinium administration [26–28]. However, these early imaging techniques were limited by long acquisition times, artifacts, and insufficient contrast between normal and abnormal regions. With faster imaging sequences using k-space segmentation, LGE can be performed in a single breath-hold with collection of data during the diastolic phase of the cardiac cycle when there is less cardiac motion. Implementation of an inversion recovery pulse sequence with inversion time set to null normal myocardium increases the signal difference between normal and infarcted segments by 500–1000% [3].

Using this approach, Kim et al. demonstrated that the spatial extent of LGE seen on CMR closely mirrored the



Fig. 10.2 4-chamber long-axis phase-sensitive inversion recovery image obtained 15 min after gadolinium administration in a patient with a prior anterior MI. Note the 75% transmural LGE in the apical septum and apex

distribution of myocyte necrosis in the early period following infarction and that of collagenous scar seen at 8 weeks ($R = 0.97$, $P < 0.001$) [4], while in regions of the heart subjected to *reversible* injury, the retention of contrast did *not* occur [29]. LGE accurately delineates infarction as defined by histology at various time points following injury [30]. When compared to other noninvasive techniques, LGE is more reliable in detecting infarct scar. In a study of 91 patients with suspected or known CAD, Wagner et al. performed both LGE and SPECT imaging to evaluate the location, extent, and size of infarction [31]. Although SPECT correctly identified all patients with transmural or near-transmural scar seen on LGE, SPECT failed to correctly identify nearly half of those with subendocardial infarction. SPECT is less sensitive to smaller, non-Q wave, primarily inferior infarcts [32]. Klein et al. compared LGE to PET in 31 patients with ischemic heart failure [33]. Infarct mass correlated well between the two modalities ($r = 0.81$, $p < 0.0001$), but LGE more frequently identified scar than PET, again reflecting the superior spatial resolution of CMR.

Transmural extent of infarct scar, as determined by LGE, is a powerful predictor of functional recovery following acute MI. Choi et al. performed LGE-CMR on 24 patients within 7 days of successful revascularization post-MI [34]. Scans were repeated at 8–12 weeks to assess functional recovery. There was an inverse relationship between transmural extent of infarction and segmental recovery of function ($p = 0.001$). Moreover, the best predictor of improved

wall thickening and global function was the extent of dysfunctional myocardium that was either without LGE or had $<25\%$ transmural LGE.

Investigators have exploited the enhanced sensitivity of CMR to study small infarctions after both percutaneous intervention [35, 36] and coronary artery bypass surgery [37]. Ricciardi et al. utilized LGE to demonstrate the etiology of CK-MB release following successful elective percutaneous coronary intervention (PCI) [36]. Fourteen patients without evidence of prior MI were imaged following elective PCI. Nine experienced elevation of cardiac enzymes following the procedure while five did not. In all patients with an enzyme leak (median CK-MB was 21 ng/mL), a discrete area of LGE was seen in the target vessel zone indicating periprocedural MI. This LGE persisted in all but one of the patients at follow-up scan 3–12 months later, while LGE was not detected in any control patient.

It should be noted that infarct size is dynamic. Measurement of infarct size histologically or with LGE demonstrates a peak in infarct size within the first few days after MI, followed by a gradual decline until 4–6 weeks after the event, after which infarct size is generally stable [38]. Infarct size in a representative canine MI study was 41% of LV size at 4 days but only 11% of LV size at 28 days. Histological examination revealed a 25% increase in water content within the acute infarct at 4 days, with dense scarring and decreased water content after 28 days [23]. In humans, infarct size has been shown to decrease by 25–30% over the first 8–12 weeks post-MI as evidenced by the decline in size of late gadolinium enhancement [39–42]. Early on after MI, the increase in infarct size is likely due to an increase in interstitial edema and necrotic cellular debris, whereas chronic infarcts are characterized by dense scarring with an increase in collagen deposition and loss of cellular structure and edema. In both acute and chronic infarcts, there is an increase in extracellular space, which causes an increased volume of distribution for gadolinium and thus increased signal intensity.

Recent evidence suggests LGE may be a valuable tool for predicting major adverse cardiac events (MACE). In a study by Kwong et al., 195 patients were evaluated for LGE as part of an assessment for CAD [43]. After 16 months of follow-up, LGE was found to be the strongest predictor of MACE (hazard ratio (HR) 8.3) and cardiac mortality (HR 10.9), even after adjustment for other clinical variables. This was true even for those patients with smaller regions of LGE (lowest tertile), as they had a sevenfold increase in MACE. Another study of 857 patients followed for 4.4 years showed that the scar index as defined by LGE predicted a composite endpoint of all-cause mortality or cardiac transplantation (HR 1.26) [44]. Those with LGE showed worse outcome over time, similarly to those with reduced LV function. A study of 349 patients with ischemic cardiomyopathy

followed for 2.6 years demonstrated that quantified scar burden above the median predicted events (51 deaths and 5 transplants) with a relative risk of 1.75 [45].

Microvascular Obstruction

In the acute phase of infarction, typically at the subendocardial core, there is often microvascular obstruction (MO). MO may result from microembolization and platelet activation as well as capillary bed compression due to edema, although the exact mechanisms are unclear [46]. These events may be exacerbated by reperfusion itself. These areas are generally devoid of blood flow and have also been described as “no-reflow zones” with the extent of no-reflow related to total infarct size [47]. The region surrounding areas of no-reflow is often comprised of myocytes subjected to significant, but varying, degrees of ischemic injury. Many undergo necrosis with loss of membrane integrity and depletion of cellular energy stores [48]. In this acute phase, tissue edema, hemorrhage, and inflammation can increase infarct volume by as much as 25% [23].

The time course of MO is an important factor in understanding the acuity of MI. Several studies have shown that the extent of MO usually peaks from 2 h to 2 days after reperfusion occurs [49–51], after which it tends to be stable in size until at least day 9 [52]. Thereafter areas of MO involute and regress and are rarely seen on follow-up CMR beyond 1–2 months after MI. Because of the timing of MO, techniques performed at the time of intervention are likely to underestimate the final extent of MO. CMR thus offers a potential advantage in that it can measure MO up to 7–10 days after infarction with good spatial resolution and without dependence on acoustic windows.

MO can be assessed by CMR using two separate techniques. Early MO is visualized early after first-pass perfusion. Typical protocols using this method define MO as hypoenhancement within the first 2–5 min after contrast injection either on first-pass perfusion imaging or on inversion recovery T1-W imaging. The second technique is LGE images 10–20 min after contrast injection and appears as an area or areas of hypoenhancement encompassed within the core of LGE, often extending from the subendocardium. This latter method is termed persistent or late MO (Fig. 10.3). The prevalence of early and late MO based on a systematic review was 65% and 54%, respectively [53]. Some of the variability between studies is due to differences in study populations, imaging methods, and timing of imaging.

There is still no consensus on whether early or late MO should be the preferred technique for evaluating MO. The spatial extent of early MO correlates well with histology and myocardial contrast echo [52]. A study of 17 patients on day 4 post-MI demonstrated that regions with early MO were nonviable as no recovery of function was noted at 7 weeks



Fig. 10.3 Short-axis phase-sensitive inversion recovery image obtained 15 min after gadolinium administration in a patient with a recent anteroseptal MI. Within the 100% transmural LGE in the anteroseptum, an area of MO is clearly seen

post-MI in these territories [54]. Early MO has been shown to be predictive of LV function and remodeling at 1-year follow-up and was a better marker of 1-year infarct size than late MO [55]. However, both early and late MO are also associated with more shrinkage of infarct size at long-term follow-up compared to those patients without MO [42].

Wu et al. found that early MO predicts infarct transmural-ity, LV function, and remodeling after 16 months and was also a powerful independent prognostic indicator of hard cardiac events even after controlling for infarct size [2]. In a study of 60 MI patients undergoing CMR at 5 days and 4 months, both early and late MO correlated with poor ST-segment resolution; however, neither method correlated well with angiographic parameters of TIMI flow grade or angiographic blush grade [56]. Late MO does, however, correlate with invasive coronary flow velocity measures of microvascular obstruction [57]. However, a meta-analysis suggested that early MO only shows a trend toward prediction of cardiac mortality, recurrent MI, and heart failure hospitalization [53].

Late MO predicts follow-up LV function and remodeling better than early MO and lends additional prognostic information beyond that of infarct size or transmural-ity. In a study by Nijveldt et al., 63 acute MI patients who received PCI and optimal medical management were assessed for early, mid-, and late MO 4–7 days after MI and followed up with CMR at 4 months. They found that late MO was a better predictor of follow-up LV ejection fraction, LV end-diastolic volume, and LV end-systolic volume than early MO [58]. In a study of 110 MI patients, Hombach et al. found that late MO independently portended an increase in cardiac events at 8-month follow-up

and gave additional prognostic information over and above infarct size alone [59]. This was corroborated in a study by Bruder et al. of 67 STEMI patients followed for 14 months which showed that late MO was a better predictor of adverse cardiac events than infarct size or baseline ejection fraction. The meta-analysis mentioned above has demonstrated that late MO has a strong relationship with both LV remodeling and major cardiac adverse events including cardiac death, recurrent MI, and heart failure hospitalization [53]. A study by Cochet et al. that directly compared the 2 methods in 187 patients showed that late MO had a hazard ratio over 3x that of early MO for prediction of MACE [60].

Recent larger clinical studies underscore the prognostic importance of MO. A multicenter study of 738 STEMI patients demonstrated that independent predictors of MACE included MO and TIMI risk score [61]. Both MO and infarct size improved prognostication over and above clinical risk and LVEF with an increase in the C-statistic from 0.76 to 0.80, $p < 0.04$.

A pooled analysis of 1025 patients with STEMI followed for 2 years showed that MO was an independent predictor of MACE with a HR of 3.74, whereas infarct size was not [62].

T2-Weighted Imaging

An understanding of the time course of edema after cardiac injury is a major key to the accurate interpretation of T2-W imaging (Fig. 10.4). Abdel-Aty et al. noted in a canine model

of myocardial infarction that the onset of edema on CMR first became apparent 28 ± 4 min after experimental coronary artery occlusion and well before the appearance of LGE or troponin elevation, signifying that CMR can visualize edema before the onset of irreversible myocardial injury [63]. Microsphere analysis in a canine model of reperfused acute MI suggested that T2-W imaging performed 2 days post-MI can be used to delineate the area at risk (AAR) [64].

The persistence of increased T2 signal post-MI has been variable across studies. A study of ten patients with transmural ST-elevation MI found that myocardial T2 signal persisted a median of 6 months after the event, with three of the ten cases persisting out to 1 year, although even in these cases, the extent and intensity of the T2 signal diminished over time [65]. Larger studies have shown that increased myocardial T2 signal after an ischemic event gradually dissipates over 1–3 months [5]. In the first 2–4 weeks after MI, the edematous area at risk of patients or experimental animals, as determined by T2-W CMR or histology, is nearly always transmural [66, 67]; however, multiple studies have noted that T2 signal resolves early on in the epicardium, whereas persistent T2 signal, if present, is often limited to the endocardial surface and may represent changes in myocardial structure from the infarct itself [5, 65].

When used in conjunction with late gadolinium-enhanced CMR, T2-W imaging confers the ability to differentiate acute from chronic infarcts. This was demonstrated in a study by Abdel-Aty et al. [5] who used LGE and T2-W CMR to evaluate 58 patients with either acute or chronic infarction.

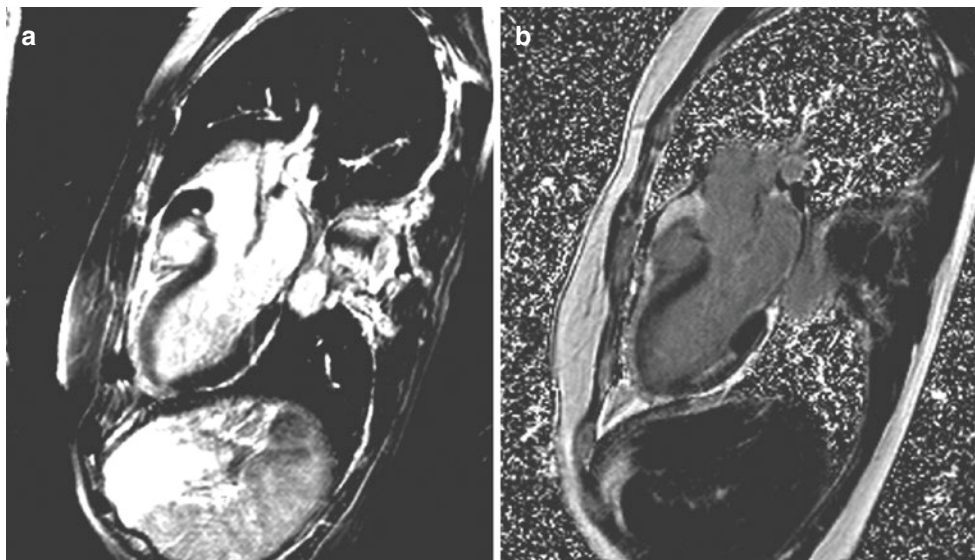


Fig. 10.4 (a) 3-chamber long-axis hybrid turbo spin echo-SSFP bright-blood T2-W image demonstrating anteroapical high signal intensity consistent with edema in a patient with chest pain, elevated troponins, and transiently occluded LAD from a coronary artery dissection. (b) 3-chamber long-axis phase-sensitive inversion recovery image

obtained 15 min after gadolinium administration in the same patient demonstrating absent LGE in the anteroapex but evidence of a prior 50% transmural inferior MI. The patient subsequently demonstrated complete recovery of function in the anteroapex

Blinded observers were able to differentiate acute from chronic infarction with specificity between 92% and 100% and sensitivity between 91% and 94%, depending on the observer.

There are several potential limitations of traditional T2-W imaging [68]. These limitations cause some investigators to urge against using T2-W imaging as a surrogate for area at risk [69]. Firstly, the T2-W signal intensity is dependent on proximity to the phased array coil. This leads to a propensity to overestimate edema in myocardium close to the chest wall due to its brighter signal and to underappreciate the T2-W signal from more distant structures. Another potential shortcoming with currently employed dark blood T2-W sequences is that slow-flowing blood appears bright, making it difficult at times to discern between a true increase in subendocardial T2 signal and blood pool artifact. Bright-blood approaches have been used, and some studies suggest improved accuracy for identifying the culprit coronary artery as well as AAR [70]. Finally, T2-W imaging tends to be sensitive to motion. Experimental protocols have used T2 mapping to overcome these limitations [68] and have been applied successfully in animal models [71].

The ability for T2-W imaging to determine the area at risk (AAR) and LGE to identify necrotic regions enables the calculation of the difference as the area of salvaged myocardium after reperfusion. Validation studies have been performed in canine models to demonstrate the ability of T2 mapping to delineate the AAR as defined by microspheres [72]. This concept has now been applied to clinical studies of acute MI. A study of 50 consecutive patients demonstrated a strong relationship of the MR assessment of AAR using a T2-prepared SSFP sequence and angiographic measures of myocardial salvage [73]. Eitel et al. studied 208 patients with

acute STEMI who underwent primary PCI and used CMR with T2-W imaging and LGE to calculate myocardial salvage [74]. They showed that patients with myocardial salvage index below the median had a higher MACE rate (22.1%) over 6-month follow-up than those with an index \geq the median (2.9%). In fact, myocardial salvage index was the strongest predictor of MACE, outperforming MO and infarct size. When follow-up of these same patients was continued over 18 months, mortality was shown to be significantly reduced in the group with salvage less than the median (2 vs. 12 deaths, $p < 0.001$) [75].

Native T1 and Post-Contrast T1 Mapping

T1 in the myocardium can be measured by mapping with a modified Look-Locker inversion (MOLLI) recovery sequence. So-called native T1 can be measured before contrast infusion (Fig. 10.5), and then post-contrast T1 measures can be used to calculate extracellular volume fraction in the myocardium. The first application of T1 mapping in 24 patients with MI demonstrated that native T1 maps detected areas of regional wall motion abnormalities with high accuracy [76]. The agreement between T1 maps and LGE was higher in chronic than acute MI. This finding was validated in a canine model that showed that T1 maps overestimated infarct size in acute MI but not in chronic MI [7]. T1 mapping has been demonstrated to be equivalent to T2-W imaging for detecting myocardial injury in patients with ST-elevation MI and superior to T2-W imaging for non-ST-elevation MI [77]. In the latter study, the higher the native T1 values, the lower the likelihood of functional recovery at 6 months post-MI. A study of post-contrast T1 times in

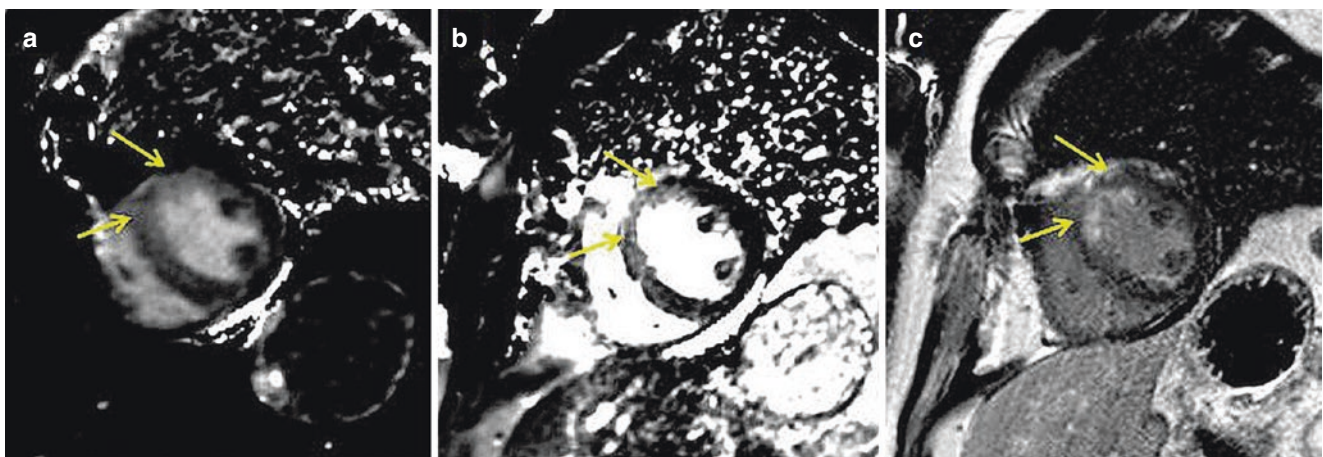


Fig. 10.5 (a) Short-axis native (pre-contrast) T1 map from a MOLLI acquisition in a patient after reperfused anterior MI. Note the transmural high T1 signal in the anteroseptum. (b) Corresponding short-axis T2-prep-based T2 map in the same patient showing transmural high T2

signal in the same region. Both the T1 and T2 maps demonstrate the area at risk. (c) LGE image in the same patient demonstrates 50% transmural enhancement, significantly smaller than the area at risk demonstrated on the T1 and T2 maps

patients with acute MI showed lower post-contrast T1 times in remote noninfarcted regions associated with reductions in wall thickening compared to controls, suggesting a contribution to LV remodeling in those regions [78].

T2*-W Imaging and Intramyocardial Hemorrhage

Intramyocardial hemorrhage (IMH) often follows MO development in the core of an infarct with a tendency to expand for several hours post-reperfusion (Fig. 10.6). It is caused by vascular endothelial damage and accumulation of red blood cells in the myocardial extracellular space [48]. It is unclear whether IMH is the cause or result of severe ischemia-reperfusion injury [79]. A high correlation between infarct size (IS) and IMH has been identified on histopathologic studies [48]. In most studies IMH is identified only in the presence of MO. The correlation (r^2) of IMH has been reported to be 0.55 with early MO and between 0.8 and 0.95 for late MO [80–82].

IMH can confound the assessment of myocardial edema and AAR as it causes a change in the T2 signal. Hemorrhage can have variable effects on the MR signal depending upon the acuity of the event, but within the first week following MI, the paramagnetic effect of iron in deoxyhemoglobin usually predominates. This causes a decrease in both T2 and T2*, resulting in signal loss and potential underestimation of the AAR. A CMR study of 70 STEMI patients demonstrated that significant T2-W signal dropout within the infarct core was sufficient to impair threshold-based assessment of the area at risk in 11% [83]. Thus, boundary detection methods for quantitative assessment of edema are probably more accurate than thresholding methods in this setting.

Most studies have used T2-W short-tau inversion recovery (STIR) or T2*-W gradient echo pulse sequences [6] to assess for IMH. T2*-W imaging is felt to be more sensitive for detection of IMH but has lower signal to noise than T2-W images and is more sensitive to off-resonance artifacts. T2* values are lowest acutely in the IMH core but gradually

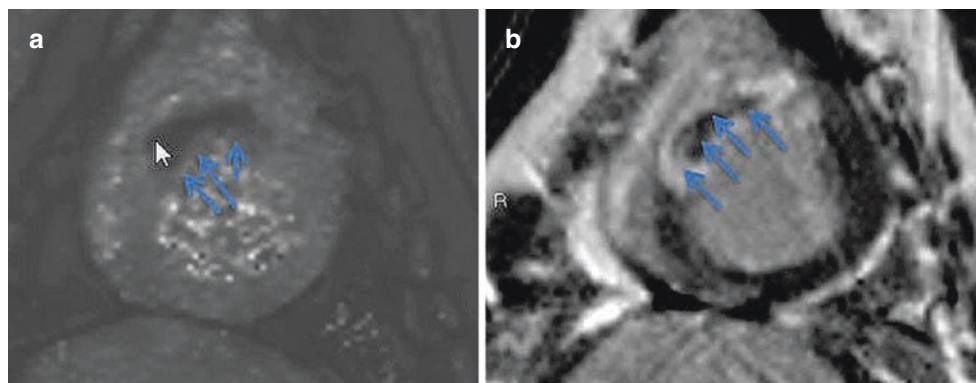
normalize to that of the rest of the infarct at 4 weeks, due to extensive collagen deposition and absence of iron [84]. A recent study in 14 STEMI patients and in 20 canines with acute reperfused myocardial infarction suggests that T2* is more suitable than T2 imaging in the identification of IMH [85]. The T2* dropped on average 54% in hemorrhagic infarctions and was 6% higher in nonhemorrhagic infarctions as compared to remote myocardium. By comparison, T2 was increased by 17% in hemorrhagic infarcts and by 38% in nonhemorrhagic infarcts.

A meta-analysis including 9 studies and 1106 patients demonstrated that IMH is associated with increased infarct size, larger LV end-diastolic and end-systolic volumes, and reduced EF compared to those without IMH [53]. IMH was seen predominantly in anterior infarcts [86] and in infarcts involving >80% of LV thickness [87]. One study of 48 patients found an independent correlation of IMH with LV remodeling and a significant improvement of diagnostic area under the curve (from 0.699 to 0.826) by adding IMH to a multivariate model including LVEF and infarct size [88]. Three studies, using T2 STIR including a total of 991 patients with a follow-up of 6 months to 3 years, examined the impact of IMH on adverse cardiovascular outcomes [80, 89, 90]. The pooled univariate hazard ratio for IMH for predicting MACE was 3.88. One study that compared the graded impact of no MO, MO only, and MO with IMH on LV remodeling or MACE detected a strong incremental association [89]. Thus there is likely a spectrum between MO and MO with IMH, with the presence of IMH suggesting greater cellular damage resulting in greater adverse remodeling and poorer outcomes.

Assessment of the Infarct Border Zone

A number of studies have used different methodologies to identify the border zone of acute MI that is thought to be associated with higher risk of ventricular tachyarrhythmias and mortality. One study investigated patients with ischemic cardiomyopathies referred for implantable cardiac defibrillators

Fig. 10.6 (a) Short-axis T2*-weighted image from a porcine model of reperfused MI demonstrating intramyocardial hemorrhage in the anteroseptum. (b) Short-axis phase-sensitive inversion recovery LGE image in the same animal demonstrating transmural LGE with a midwall region of intramyocardial hemorrhage



(ICD) in order to determine if heterogeneity in peri-infarct regions can be established using contrast-enhanced CMR with the idea that adjacent areas of necrosis and viable myocardium could be fertile ground for reentrant arrhythmias [91]. The infarct core was defined as myocardium with signal intensity greater than 50% maximum. Tissue heterogeneity in the infarct periphery or “gray zone” was defined as having signal intensity greater than that of remote myocardium but less than 50% of the maximum. The region of intermediate late gadolinium enhancement, characterized as the “gray zone” at the periphery of myocardial scar, was related to inducibility of monomorphic ventricular tachycardia [91].

Yan et al. tested the hypothesis that the degree of gray zone measured by contrast-enhanced CMR would be an independent predictor of mortality post-MI [92]. In this study, the total infarct size was measured semiquantitatively and divided into the core region (>3 SD above normal remote myocardium) and the gray zone or peri-infarct regions (with signal intensity between 2 and 3 SD above normal myocardium). The peri-infarct zone was then normalized as a percentage of total infarct size. After adjusting for age and LVEF, the normalized peri-infarct zone was independently associated with all-cause and CV mortality (adjusted HR, 1.42 and 1.49, respectively).

Another study evaluated patients with ischemic cardiomyopathy referred for ICD by contrast-enhanced CMR to establish a relationship between extent of peri-infarct gray zone and spontaneous ventricular arrhythmia [93]. Roes et al. found the presence of peri-infarct tissue heterogeneity on contrast-enhanced MRI in patients with prior MI to be a stronger predictor of spontaneous ventricular arrhythmia and ICD therapy when compared to total infarct size and LV function. Thus, gray zone may ultimately be useful in choosing post-MI patients for ICD therapy.

There are several limitations of the “gray zone” approach. One is that there is significant concern in regard to difficulty measuring the gray zone in that it suffers from inadequate spatial resolution of LGE imaging and thus partial volume effects at the border of normal and infarcted myocardium [94]. In addition, there is as of yet no standardization between laboratories of methodologies used to measure the area of “gray zone.” In fact, of the three manuscripts discussed above, each used a completely independent method to make this measurement. The assessment of “gray zone” will require standardization before it can move forward and be clinically useful.

Detection of Infarct Complications

Due to its high spatial resolution and ability to differentiate tissue types, CMR can readily detect ventricular wall pathology such as ventricular septal defects (Fig. 10.7), or free wall aneurysms, and can differentiate aneurysm from pseudoan-

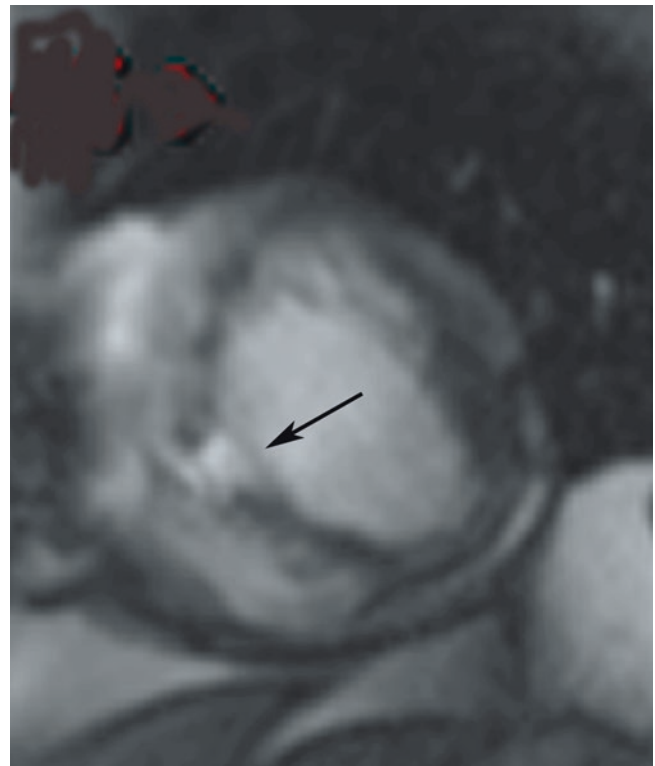


Fig. 10.7 Short-axis SSFP image at end diastole in a patient after non-reperfused anteroapical MI demonstrating an apical VSD (black arrow)

eurysm (Fig. 10.8) [95], with its accompanying treatment implications. Right ventricular infarction is also very well visualized by LGE-CMR [96].

Visualization of LGE within the papillary muscles is indicative of infarction and has been reported in post-MI CMR studies to occur in 26–53% of patients [59, 97]. In a study of 60 patients with old MI, bilateral papillary muscle infarction was seen by LGE in 17% of cases and was associated with a higher incidence of severe mitral regurgitation and LV remodeling than in those with unilateral or no papillary muscle infarction [97]. Mitral leaflet LGE has been seen more commonly in post-MI patients [98].

Inflammatory pericarditis is visualized by LGE of the pericardium with high sensitivity and specificity after MI [99] and has been reported to occur in as many as 40% of STEMI patients [59]. High T2-W signal can be visualized in inflammatory pericarditis [100], although this has not been studied specifically in post-MI patients.

The presence of intraventricular thrombi has been reported in 7–29% of patients with decreased ejection fraction, depending on the population studied [101, 102], and is associated with a higher risk of thromboembolic events, including stroke [101, 103]. The most prominent risk factors for the development of LV thrombus include anterior infarction (Fig. 10.9), infarct size, LV aneurysm, and decreased ejection fraction ($\leq 40\%$) [102, 104]. Contrast-enhanced (LGE) CMR

Fig. 10.8 (a) A 2-chamber long-axis SSFP cine image at end diastole in a patient 5 years after anterior MI demonstrating a chronic anterior pseudoaneurysm. (b) Short-axis phase-sensitive inversion recovery LGE image from the same patient demonstrating enhancement of the fibrous outer layer of the pseudoaneurysm which is lined with thrombus which appears black

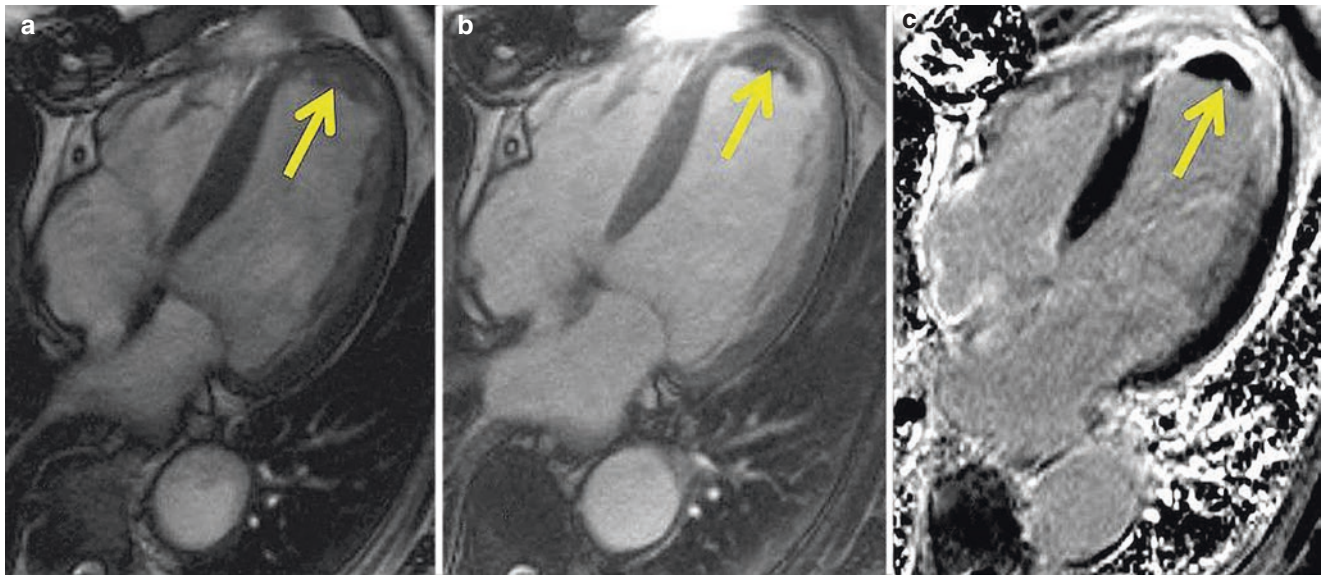
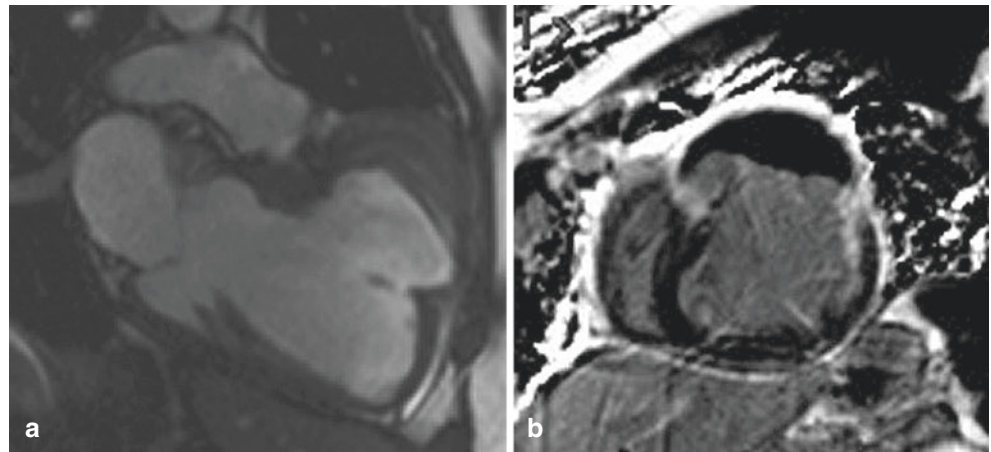


Fig. 10.9 (a) 4-chamber long-axis cine steady-state free precession (SSFP) image in a patient after late reperfusion of an anterior MI. Prior to contrast, it is difficult to discern whether there is thrombus in the apex. (b) Post-contrast 4-chamber SSFP image provides greater con-

trast between the slightly enhancing myocardium and nonenhancing thrombus at the apex. (c) LGE imaging clearly demonstrates the black thrombus at the apex adjacent to the transmural apical infarct

has been shown to more accurately diagnose thrombi within the LV than transthoracic echocardiography or transesophageal echocardiography. In a multimodality imaging study of 361 patients with ischemic cardiomyopathy undergoing cardiac surgery, the presence of LV thrombus by LGE-CMR, TTE, and TEE was compared to pathology and was found to have sensitivities and specificities of 88% and 99% for LGE, 23% and 96% for TTE, and 40% and 96% for TEE, respectively [101]. While contrast echocardiography nearly doubles the sensitivity of non-contrast echo, mural and small apical LV thrombi are still frequently missed [102]. Recently, the use of prolonged inversion times (600 ms) during LGE imaging has been shown to increase the sensitivity of LGE for detecting thrombus [102]. Post-contrast SSFP cine imaging can be quite useful as well in this regard (Fig. 10.9).

Post-MI LV Remodeling

After MI, the LV undergoes a series of adaptive and maladaptive changes [105], proportional to the size and transmural extent of the infarct, which extend well beyond the infarcted segment. Remodeling in the early post-MI period is characterized by infarct expansion and thinning, with subsequent cavity dilation in the infarcted area due to weakening of the infarct from myocyte slippage and loss [106, 107]. Over time, the necrotic, infarcted myocardium is replaced by fibrous scar, while adjacent viable segments undergo eccentric hypertrophy [19] and fibrous deposition [108] causing global increases in ventricular volumes and worsened mechanical function (Fig. 10.10) [20]. Although these changes attempt to restore stroke volume and cardiac

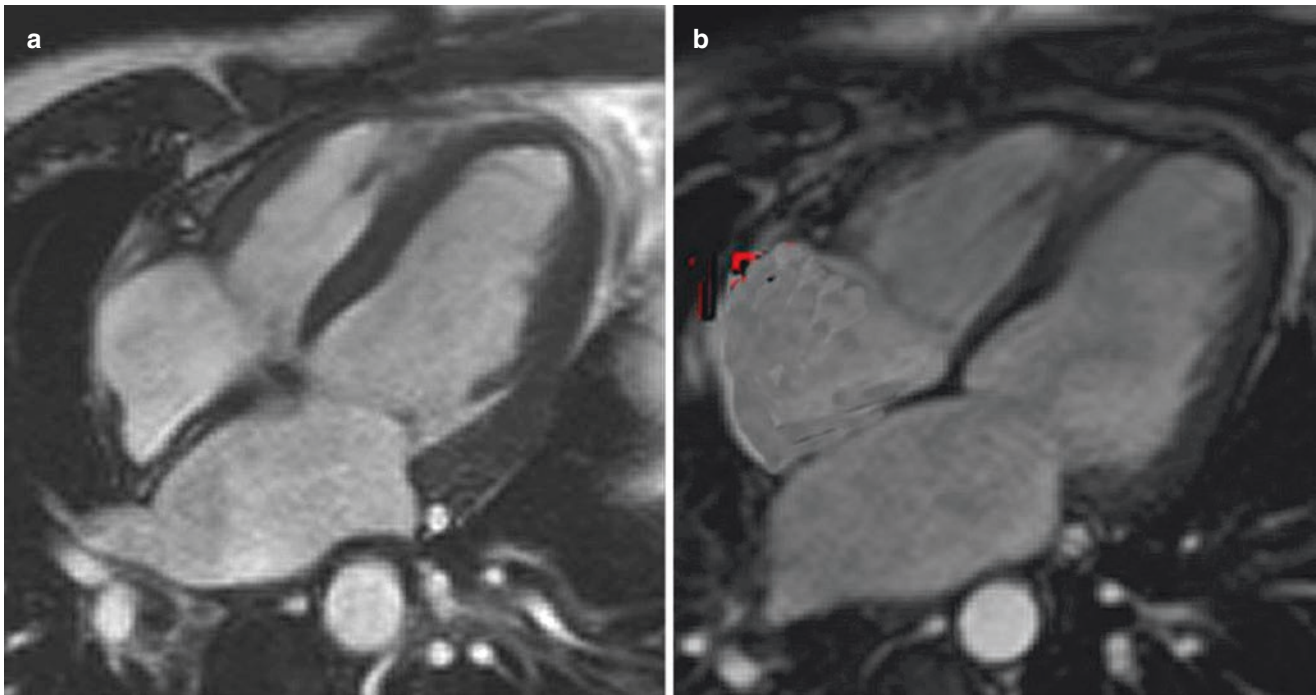


Fig. 10.10 (a) 4-chamber long-axis SSFP cine image in a patient 3 days after anterior MI. (b) 4-chamber long-axis SSFP cine image in the same patient 6 months later. Note the interval dilation of the LV consistent with adverse remodeling as well as dilation of the RV and both atria

output, they are associated with worsened mortality [12, 109]. Therapies which successfully attenuate post-MI remodeling have been shown to improve outcomes.

Because of its marked prognostic significance after MI, there is substantial interest in finding accurate predictors of remodeling which can be assessed at the time of MI. Baseline measurements of left ventricular function and volumes are a tempting target, and baseline ejection fraction and LV volumes have been shown to be modestly predictive of remodeling on follow-up [110]. However, due to the remodeling process and the frequent presence of stunned, but viable, myocardium in the peri-infarct area [111], measurements of systolic performance immediately post-MI are inherently unreliable. Clinical parameters, such as the ST-segment resolution and the time from symptom onset to reperfusion, have also been shown to be associated with poor LV function at follow-up [112] but are also relatively poor and indirect markers of follow-up function. Multiple studies have demonstrated that several CMR-based parameters are much better predictors of long-term LV remodeling. In a study of 73 STEMI patients in whom CMR was performed within 1 week and again 3 months after MI, infarct size, as measured by LGE, was shown to be a better determinant of follow-up EF than was the baseline EF [113]. Larose et al. confirmed this finding in a study of 103 STEMI patients, demonstrating that infarct size was the most powerful predictor of 6-month LV dysfunction, with an area under the receiver-operator characteristic curve of 0.92 for infarct size,

compared to 0.84, 0.79, and 0.71 for baseline ejection fraction, peak enzyme elevation, and time from symptom onset to revascularization, respectively [110].

Microvascular obstruction (MO) as a marker for subsequent remodeling was first demonstrated angiographically [114], and CMR-based assessment of MO has since been shown to be a powerful predictor of poor LV function, as discussed earlier in this chapter. MO and IMH directly relate to poor functional recovery and adverse LV remodeling [115]. Myocardial salvage index is a relatively recent measure for predicting post-MI prognosis, but initial studies are very promising. In a study of 137 reperfused acute STEMI patients, MSI was shown to be more predictive of adverse LV remodeling at 4 months than infarct size, MO, or traditional measures of prognosis [116]. Therapies that limit reperfusion injury and thus limit MO and IMH and maximize myocardial salvage will prevent subsequent adverse remodeling.

References

1. Kramer CM, Rogers WJ, Geskin G, Power TP, Theobald TM, Hu YL, et al. Usefulness of magnetic resonance imaging early after acute myocardial infarction. *Am J Cardiol.* 1997;80(6):690–5.
2. Wu KC, Zerhouni EA, Judd RM, Lugo-Olivieri CH, Barouch LA, Schulman SP, et al. Prognostic significance of microvascular obstruction by magnetic resonance imaging in patients with acute myocardial infarction. *Circulation.* 1998;97(8):765–72.

3. Simonetti OP, Kim RJ, Fieno DS, et al. An improved MR imaging technique for the visualization of myocardial infarction. *Radiology*. 2001;218:215–23.
4. Kim RJ, Fieno DS, Parrish TB, Harris K, Chen E-L, Simonetti O, et al. Relationship of MRI delayed contrast enhancement to irreversible injury, infarct age and contractile function. *Circulation*. 1999;100:1992–2002.
5. Abdel-Aty H, Zagrosek A, Schulz-Menger J, Taylor AJ, Messroghli D, Kumar A, et al. Delayed enhancement and T2-weighted cardiovascular magnetic resonance imaging differentiate acute from chronic myocardial infarction. *Circulation*. 2004;109(20):2411–6.
6. Kumar A, Green JD, Sykes JM, Ephrat P, Carson JLL, Mitchell AJ, et al. Detection and quantification of myocardial reperfusion hemorrhage using T2*-weighted CMR. *JACC Cardiovasc Imaging*. 2011;4(12):1274–83.
7. Kali A, Cokic I, Tang RLQ, Yang HJ, Sharif B, Marbán E, et al. Determination of location, size, and transmural extent of chronic myocardial infarction without exogenous contrast media by using cardiac magnetic resonance imaging at 3 T. *Circ Cardiovasc Imaging*. 2014;7(3):471–81.
8. Hundley WG, Bluemke DA, Finn JP, Flamm SD, Fogel MA, Friedrich MG, et al. ACCF/ACR/AHA/NASCI/SCMR 2010 expert consensus document on cardiovascular magnetic resonance: a report of the American College of Cardiology Foundation task force on expert consensus documents. *J Am Coll Cardiol*. 2010;55(23):2614–62.
9. Hunt SA, Abraham WT, Chin MH, Feldman AM, Francis GS, Ganiats TG, et al. 2009 focused update incorporated into the ACC/AHA 2005 guidelines for the diagnosis and management of heart failure in adults: a report of the American College of Cardiology Foundation/American Heart Association Task Force on practice guidelines developed in collaboration with the International Society for Heart and Lung Transplantation. *J Am Coll Cardiol*. 2009;53(15):e1–e90.
10. Hendel RC, Patel MR, Kramer CM, Poon M, Hendel RC, Carr JC, et al. ACCF/ACR/SCCT/SCMR/ASNC/NASCI/SCAI/SIR 2006 appropriateness criteria for cardiac computed tomography and cardiac magnetic resonance imaging: a report of the American College of Cardiology Foundation Quality Strategic Directions Committee Appropriateness Criteria Working Group, American College of Radiology, Society of Cardiovascular Computed Tomography, Society for Cardiovascular Magnetic Resonance, American Society of Nuclear Cardiology, North American Society for Cardiac Imaging, Society for Cardiovascular Angiography and Interventions, and Society of Interventional Radiology. *J Am Coll Cardiol*. 2006;48(7):1475–97.
11. The Multicenter Postinfarction Research Group. Risk stratification and survival after myocardial infarction. *N Engl J Med*. 1983;309(6):331–6.
12. White HD, Norris RM, Brown MA, Brandt PW, Whitlock RM, Wild CJ. Left ventricular end-systolic volume as the major determinant of survival after recovery from myocardial infarction. *Circulation*. 1987;76(1):44–51.
13. Isbell DC, Kramer CM. Cardiovascular magnetic resonance: structure, function, perfusion, and viability. *J Nucl Cardiol*. 2005;12:324–36.
14. Grothues F, Smith GC, Moon JCC, Bellenger NG, Collins P, Klein HU, et al. Comparison of interstudy reproducibility of cardiovascular magnetic resonance with two-dimensional echocardiography in normal subjects and in patients with heart failure or left ventricular hypertrophy. *Am J Cardiol*. 2002 Jul 1;90:29–34.
15. Bellenger NG, Davies LC, Francis JM, Coats AJS, Pennell DJ. Reduction in sample size for studies of remodeling in heart failure by the use of cardiovascular magnetic resonance. *J Cardiovasc Magn Reson*. 2000;2(4):271–8.
16. Zerhouni EA, Parish DM, Rogers WJ, Yang A, Shapiro EP. Human heart: tagging with MR imaging: a new method for noninvasive assessment of myocardial motion. *Radiology*. 1988;169:59–63.
17. Kim D, Gilson WD, Kramer CM, Epstein FH. Myocardial tissue tracking with two-dimensional cine displacement-encoded MR imaging: development and initial evaluation. *Radiology*. 2004;230(3):862–71.
18. Kramer CM, Lima JAC, Reichek N, Ferrari VA, Llaneras MR, Palmon LC, et al. Regional differences in function within non-infarcted myocardium during left-ventricular remodeling. *Circulation*. 1993;88(3):1279–88.
19. Kramer CM, Rogers WJ, Theobald TM, Power TP, Petruolo S, Reichek N. Remote noninfarcted region dysfunction soon after first anterior myocardial infarction. A magnetic resonance tagging study. *Circulation*. 1996;94(4):660–6.
20. Kramer CM, Rogers WJ, Theobald TM, Power TP, Geskin G, Reichek N. Dissociation between changes in intramyocardial function and left ventricular volumes in the eight weeks after first anterior myocardial infarction. *J Am Coll Cardiol*. 1997;30(7):1625–32.
21. Azevedo CF, Amado LC, Kraitchman DL, Gerber BL, Osman NF, Rochitte CE, et al. Persistent diastolic dysfunction despite complete systolic functional recovery after reperfused acute myocardial infarction demonstrated by tagged magnetic resonance imaging. *Eur Heart J*. 2004;25(16):1419–27.
22. Sun Y, Kiani MF, Postlethwaite AE, Weber KT. Infarct scar as living tissue. *Basic Res Cardiol*. 2002;97(5):343–7.
23. Reimer KA, Jennings RB. Changing anatomic reference base of evolving myocardial-infarction – underestimation of myocardial collateral blood-flow and over-estimation of experimental anatomic infarct size due to tissue edema. *Hemorrhage Acute-Infamm Circ*. 1979;60(4):866–76.
24. Fishbein MC, Maclean D, Maroko PR. The histopathologic evolution of myocardial infarction. *Chest*. 1978;73(6):843–9.
25. Jugdutt BI, Amy RW. Healing after myocardial infarction in the dog: changes in infarct hydroxyproline and topography. *J Am Coll Cardiol*. 1986;7(1):91–102.
26. Rehr RB, Peshock RM, Malloy CR, Keller AM, Parkey RW, Buja LM, et al. Improved in vivo magnetic resonance imaging of acute myocardial infarction after intravenous paramagnetic contrast agent administration. *Am J Cardiol*. 1986;57(10):864–8.
27. Peshock RM, Malloy CR, Buja LM, Nunnally RL, Parkey RW, Willerson JT. Magnetic resonance imaging of acute myocardial infarction: gadolinium diethylenetriamine pentaacetic acid as a marker of reperfusion. *Circulation*. 1986;74(6):1434–40.
28. de Roos A, Doornbos J, van der Wall EE, Van Voorthuisen AE. MR imaging of acute myocardial infarction: value of Gd-DTPA. *AJR Am J Roentgenol*. 1988;150(3):531–4.
29. Rehwald WG, Fieno DS, Chen EL, Kim RJ, Judd RM. Myocardial magnetic resonance imaging contrast agent concentrations after reversible and irreversible ischemic injury. *Circulation*. 2002;105(2):224–9.
30. Fieno DS, Kim RJ, Chen EL, Lomasney JW, Klocke FJ, Judd RM. Contrast-enhanced magnetic resonance imaging of myocardium at risk – distinction between reversible and irreversible injury throughout infarct healing. *J Am Coll Cardiol*. 2000;36(6):1985–91.
31. Wagner A, Mahrholdt H, Holly TA, Elliott MD, Regenfus M, Parker M, Klocke FJ, et al. Contrast-enhanced MRI and routine single photon emission computed tomography (SPECT) perfusion imaging for detection of subendocardial myocardial infarcts: an imaging study. *Lancet*. 2003;361:374–9.
32. Ibrahim T, Bulow HP, Hackl T, Hornke M, Nekolla SG, Breuer M, et al. Diagnostic value of contrast-enhanced magnetic resonance imaging and single-photon emission computed tomography for detection of myocardial necrosis early after acute myocardial infarction. *J Am Coll Cardiol*. 2007;49(2):208–16.
33. Klein C, Nekolla SG, Bengel FM, Momose M, Sammer A, Haas F, et al. Assessment of myocardial viability with contrast-enhanced magnetic resonance imaging: comparison with positron emission tomography. *Circulation*. 2002;105:162–7.

34. Choi KM, Kim RJ, Gubernikoff G, Vargas JD, Parker M, Judd RM. Transmural extent of acute myocardial infarction predicts long-term improvement in contractile function. *Circulation*. 2001;104(10):1101–7.
35. Choi JW, Gibson CM, Murphy SA, Davidson CJ, Kim RJ, Ricciardi MJ. Myonecrosis following stent placement: association between impaired TIMI myocardial perfusion grade and MRI visualization of microinfarction. *Catheter Cardiovasc Interv*. 2004;61(4):472–6.
36. Ricciardi MJ, Wu E, Davidson CJ, Choi KM, Klocke FJ, Bonow RO, et al. Visualization of discrete microinfarction after percutaneous coronary intervention associated with mild creatine kinase-MB elevation. *Circulation*. 2001;103(23):2780–3.
37. Steuer J, Bjerner T, Duvernoy O, Jideus L, Johansson L, Ahlstrom H, et al. Visualisation and quantification of peri-operative myocardial infarction after coronary artery bypass surgery with contrast-enhanced magnetic resonance imaging. *Eur Heart J*. 2004;25(15):1293–9.
38. Kim HW, Farzaneh-Far A, Kim RJ. Cardiovascular magnetic resonance in patients with myocardial infarction. *J Am Coll Cardiol*. 2009;55(1):1–16.
39. Choi CJ, Haji-Momenian S, DiMaria JM, Epstein FH, Rogers WJ, Kramer CM. Infarct involution and improved function during healing of acute myocardial infarction: the role of microvascular obstruction. *J Cardiovasc Magn Reson*. 2004;6:915–23.
40. Ingkanisorn WP, Rhoads KL, Aletras AH, Kellman P, Arai AE. Gadolinium delayed enhancement cardiovascular magnetic resonance correlates with clinical measures of myocardial infarction. *J Am Coll Cardiol*. 2004;43:2253–9.
41. Nijveldt R, Beek AM, Hofman MBM, Umans VAWM, Algra PR, Spreeuwenberg MD, et al. Late gadolinium-enhanced cardiovascular magnetic resonance evaluation of infarct size and microvascular obstruction in optimally treated patients after acute myocardial infarction. *J Cardiovasc Magn Reson*. 2007;9(5):765–70.
42. Weir RAP, Murphy CA, Petrie CJ, Martin TN, Balmain S, Clements S, et al. Microvascular obstruction remains a portent of adverse remodeling in optimally treated patients with left ventricular systolic dysfunction after acute myocardial infarction. *Circ Cardiovasc Imaging*. 2010;3(4):360–7.
43. Kwong RY, Chan AK, Brown KA, Chan CW, Reynolds HG, Tsang S, et al. Impact of unrecognized myocardial scar detected by cardiac magnetic resonance imaging on event-free survival in patients presenting with signs or symptoms of coronary artery disease. *Circulation*. 2006;113(23):2733–43.
44. Cheong BYC, Muthupillai R, Wilson JM, Sung A, Huber S, Amin S, et al. Prognostic significance of delayed-enhancement magnetic resonance imaging survival of 857 patients with and without left ventricular dysfunction. *Circulation*. 2009;120(21):2069–76.
45. Kwon DH, Halley CM, Carrigan TP, Zysek V, Popovic ZB, Setser R, et al. Extent of left ventricular scar predicts outcomes in ischemic cardiomyopathy patients with significantly reduced systolic function: a delayed hyperenhancement cardiac magnetic resonance study. *JACC Cardiovasc Imaging*. 2009;2(1):34–44.
46. Reffelmann T, Kloner RA. Microvascular alterations after temporary coronary artery occlusion: the no-reflow phenomenon. *J Cardiovasc Pharmacol Ther*. 2004;9(3):163–72.
47. Kramer CM. The prognostic significance of microvascular obstruction after myocardial infarction as defined by cardiovascular magnetic resonance. *Eur Heart J*. 2005;26(6):532–3.
48. Kloner RA, Ganote CE, Jennings RB. The “no-reflow” phenomenon after temporary coronary occlusion in the dog. *J Clin Invest*. 1974;54(6):1496–508.
49. Reffelmann T, Kloner RA. Microvascular reperfusion injury: rapid expansion of anatomic no reflow during reperfusion in the rabbit. *Am J Physiol-Heart Circ Physiol*. 2002;283(3):H1099–107.
50. Ambrosio G, Weisman HF, Mannisi JA, Becker LC. Progressive impairment of regional myocardial perfusion after initial restoration of posts ischemic blood-flow. *Circulation*. 1989;80(6):1846–61.
51. Rochitte CE, Lima JAC, Bluemke DA, Reeder SB, McVeigh ER, Furuta T, et al. Magnitude and time course of microvascular obstruction and tissue injury after acute myocardial infarction. *Circulation*. 1998;98(10):1006–14.
52. Wu KC, Kim RJ, Bluemke DA, Rochitte CE, Zerhouni EA, Becker LC, et al. Quantification and time course of microvascular obstruction by contrast-enhanced echocardiography and magnetic resonance imaging following acute myocardial infarction and reperfusion. *J Am Coll Cardiol*. 1998;32(6):1756–64.
53. Hamirani YS, Wong A, Kramer CM, Salerno M. The effect of microvascular obstruction and intramyocardial hemorrhage by CMR on left ventricular remodeling and outcomes post-MI: a systematic review and meta-analysis. *JACC Cardiovasc Imaging*. 2014;7(9):940–52.
54. Rogers WJ, Kramer CM, Geskin G, Hu YL, Theobald TM, Vido DA, et al. Early contrast-enhanced MRI predicts late functional recovery after reperfused myocardial infarction. *Circulation*. 1999;99(6):744–50.
55. Orn S, Manhenke C, Greve OJ, Larsen AI, Bonarjee VVS, Edvardsen T, et al. Microvascular obstruction is a major determinant of infarct healing and subsequent left ventricular remodeling following primary percutaneous coronary intervention. *Eur Heart J*. 2009;30(16):1978–85.
56. Nijveldt R, Beek AM, Hirsch A, Hofman MBM, Umans VAWM, Algra PR, et al. ‘No-reflow’ after acute myocardial infarction: direct visualisation of microvascular obstruction by gadolinium-enhanced CMR. *Netherlands Heart J*. 2008;16(5):179–81.
57. Hirsch A, Nijveldt R, Haeck JDE, Beek AM, Koch KT, Henriques JPS, et al. Relation between the assessment of microvascular injury by cardiovascular magnetic resonance and coronary Doppler flow velocity measurements in patients with acute anterior wall myocardial infarction. *J Am Coll Cardiol*. 2008;51(23):2230–8.
58. Nijveldt R, Hofman MBM, Hirsch A, Beek AM, Umans VAWM, Algra PR, et al. Assessment of microvascular obstruction and prediction of short-term remodeling after acute myocardial infarction: cardiac MR imaging study. *Radiology*. 2009;250(2):363–70.
59. Hombach V, Grebe O, Merkle N, Waldenmaier S, Hoher M, Kochs M, et al. Sequelae of acute myocardial infarction regarding cardiac structure and function and their prognostic significance as assessed by magnetic resonance imaging. *Eur Heart J*. 2005;26(6):549–57.
60. Cochet A, Lorgis L, Lalande A, Zeller M, Beer JC, Walker P, et al. Major prognostic impact of persistent microvascular obstruction as assessed by contrast-enhanced cardiac magnetic resonance in reperfused acute myocardial infarction. *Eur Radiol*. 2009;19(9):2117–26.
61. Eitel I, de Waha S, Wöhrle J, Fuernau G, Lurz P, Pauschinger M, et al. Comprehensive prognosis assessment by CMR imaging after ST-segment elevation myocardial infarction. *J Am Coll Cardiol*. 2014;64(12):1217–26.
62. van Kranenburg M, Magro M, Thiele H, de Waha S, Eitel I, Cochet A, et al. Prognostic value of microvascular obstruction and infarct size, as measured- δ by CMR in STEMI patients. *JACC: Cardiovasc Imaging*. 2014;7(9):930–9.
63. Abdel-Aty H, Cocker M, Meek C, Tyberg JV, Friedrich MG. Edema as a very early marker for acute myocardial ischemia a cardiovascular magnetic resonance study. *J Am Coll Cardiol*. 2009;53(14):1194–201.
64. Aletras AH, Tilak GS, Natanzon A, Hsu LY, Gonzalez FM, Hoyt RF Jr, et al. Retrospective determination of the area at risk for reperfused acute myocardial infarction with T2-weighted cardiac magnetic resonance imaging: histopathological and displacement

- encoding with stimulated echoes (DENSE) functional validations. *Circulation*. 2006;113(15):1865–70.
65. Nilsson JC, Nielsen G, Groenning BA, Fritz-Hansen T, Sondergaard L, Jensen GB, et al. Sustained postinfarction myocardial oedema in humans visualised by magnetic resonance imaging. *Heart*. 2001;85(6):639–42.
66. Karolle BL, Carlson RE, Aisen AM, Buda AJ. Transmural distribution of myocardial edema by NMR relaxometry following myocardial-ischemia and reperfusion. *Am Heart J*. 1991;122(3):655–64.
67. Friedrich MG, Abdel-Aty H, Taylor A, Schulz-Menger J, Messroghli D, Dietz R. The salvaged area at risk in reperfused acute myocardial infarction as visualized by cardiovascular magnetic resonance. *J Am Coll Cardiol*. 2008;51(16):1581–7.
68. Giri S, Chung YC, Merchant A, Mihai G, Rajagopalan S, Raman SV, et al. T2 quantification for improved detection of myocardial edema. *J Cardiovasc Magn Reson*. 2009;30:11.
69. Croisille P, Kim HW, Kim RJ. Controversies in cardiovascular MR imaging: T2-weighted imaging should not be used to delineate the area at risk in ischemic myocardial injury. *Radiology*. 2012;265(1):12–22.
70. Payne AR, Casey M, McClure J, McGeoch R, Murphy A, Woodward R, et al. Bright-blood T2-weighted MRI has higher diagnostic accuracy than dark-blood short tau inversion recovery MRI for detection of acute myocardial infarction and for assessment of the ischemic area at risk and myocardial salvage. *Circ Cardiovasc Imaging*. 2011;4(3):210–9.
71. Hammer-Hansen S. Distinction of salvaged and infarcted myocardium within the ischaemic area-at-risk with T2 mapping. *Eur Heart J Cardiovasc Imaging*. 2014;15(9):1048–53.
72. Ugander M, Bagi PS, Oki AJ, Chen B, Hsu LY, Aletras AH, et al. Myocardial edema as detected by pre-contrast T1 and T2 CMR delineates area at risk associated with acute myocardial infarction. *JACC Cardiovasc Imaging*. 2012;5(6):596–603.
73. Berry C, Kellman P, Mancini C, Chen MY, Bandettini WP, Lowrey T, et al. Magnetic resonance imaging delineates the ischemic area at risk and myocardial salvage in patients with acute myocardial infarction. *Circ Cardiovasc Imaging*. 2010;3(5):527–35.
74. Eitel I, Desch S, Fuernau G, Hildebrand L, Gutberlet M, Schuler G, et al. Prognostic significance and determinants of myocardial salvage assessed by cardiovascular magnetic resonance in acute reperfused myocardial infarction. *J Am Coll Cardiol*. 2010;52:2470–9.
75. Eitel I, Desch S, de Waha S, Fuernau G, Gutberlet M, Schuler G, et al. Long-term prognostic value of myocardial salvage assessed by cardiovascular magnetic resonance in acute reperfused myocardial infarction. *Heart*. 2011;97(24):2038–45.
76. Messroghli DR, Walters K, Plein S, Sparrow P, Friedrich MG, Ridgway JP, et al. Myocardial T1 mapping: application to patients with acute and chronic myocardial infarction. *Magn Reson Med*. 2007;58(1):34–40.
77. Dall'Armellina E, Piechnik S, Ferreira V, Si QL, Robson M, Francis J, et al. Cardiovascular magnetic resonance by non contrast T1-mapping allows assessment of severity of injury in acute myocardial infarction. *J Cardiovasc Magn Reson*. 2012;14(1):15.
78. Chan W, Duffy SJ, White DA, Gao XM, Du XJ, Ellims AH, et al. Acute left ventricular remodeling following myocardial infarction: coupling of regional healing with remote extracellular matrix expansion. *JACC Cardiovasc Imaging*. 2012;5(9):884–93.
79. Yellon DM, Hausenloy DJ. Myocardial reperfusion injury. *N Engl J Med*. 2007;357(11):1121–35.
80. Husser O, Monmeneu JV, Sanchis J, Nunez J, Lopez-Lereu MP, Bonanad C, et al. Cardiovascular magnetic resonance-derived intramyocardial hemorrhage after STEMI: influence on long-term prognosis, adverse left ventricular remodeling and relationship with microvascular obstruction. *Int J Cardiol*. 2013;167(5):2047–54.
81. Jensen C, Eberle H, Nassenstein K, Schlosser T, Farazandeh M, Naber C, et al. Impact of hyperglycemia at admission in patients with acute ST-segment elevation myocardial infarction as assessed by contrast-enhanced MRI. *Clin Res Cardiol*. 2011;100(8):649–59.
82. O'Regan DP, Ahmed R, Karunanithy N, Neuwirth C, Tan Y, Durighel G, et al. Reperfusion hemorrhage following acute myocardial infarction: assessment with T2* mapping and effect on measuring the area at risk. *Radiology*. 2009;250(3):916–22.
83. Francone M, Bucciarelli-Ducci C, Carbone I, Canali E, Scardala R, Calabrese FA, et al. Impact of primary coronary angioplasty delay on myocardial salvage, infarct size, and microvascular damage in patients with ST-segment elevation myocardial infarction insight from cardiovascular magnetic resonance. *J Am Coll Cardiol*. 2009;54(23):2145–53.
84. Robbers LFHJ, Eerenberg ES, Teunissen PFA, Jansen MF, Hollander MR, Horrevoets AJG, et al. Magnetic resonance imaging-defined areas of microvascular obstruction after acute myocardial infarction represent microvascular destruction and haemorrhage. *Eur Heart J*. 2013;34(30):2346–53.
85. Kali A, Tang RLQ, Kumar A, Min JK, Dharmakumar R. Detection of acute reperfusion myocardial hemorrhage with cardiac MR imaging: T2 versus T2*. *Radiology*. 2013;269(2):387–95.
86. Ochiai K, Shimada T, Murakami Y, Ishibashi Y, Sano K, Kitamura J, Inoue S, et al. Hemorrhagic myocardial infarction after coronary reperfusion detected in vivo by magnetic resonance imaging in humans: prevalence and clinical implication. *J Cardiovasc Magn Reson*. 1999;1:247–56.
87. O'Regan DP, Ariff B, Neuwirth C, Tan Y, Durighel G, Cook SA. Assessment of severe reperfusion injury with T2* cardiac MRI in patients with acute myocardial infarction. *Heart*. 2010;96(23):1885–91.
88. Mather AN, Fairbairn TA, Ball SG, Greenwood JP, Plein S. Reperfusion haemorrhage as determined by cardiovascular MRI is a predictor of adverse left ventricular remodelling and markers of late arrhythmic risk. *Heart*. 2011;97(6):453–9.
89. Eitel I, Kubusch K, Strohm O, Desch S, Mikami Y, de Waha S, et al. Prognostic value and determinants of a hypointense infarct core in T2-weighted cardiac magnetic resonance in acute reperfused ST-Elevation Myocardial infarction. *Circ Cardiovasc Imaging*. 2011;4(4):354–62.
90. Amabile N, Jacquier A, Shuhab A, Gaudart J, Bartoli JM, Paganelli F, et al. Incidence, predictors, and prognostic value of intramyocardial hemorrhage lesions in ST elevation myocardial infarction. *Cathet Cardiovasc Intervent*. 2012;79(7):1101–8.
91. Schmidt A, Azevedo CF, Cheng A, Gupta SN, Bluemke DA, Foo TK, et al. Infarct tissue heterogeneity by magnetic resonance imaging identifies enhanced cardiac arrhythmia susceptibility in patients with left ventricular dysfunction. *Circulation*. 2007;115(15):2006–14.
92. Yan AT, Shayne AJ, Brown KA, Gupta SN, Chan CW, Luu TM, et al. Characterization of the peri-infarct zone by contrast-enhanced cardiac magnetic resonance imaging is a powerful predictor of post-myocardial infarction mortality. *Circulation*. 2006;114(1):32–9.
93. Roes SD, Borleffs CJ, van der Geest RJ, Westenberg JJ, Marsan NA, Kaandorp TA, et al. Infarct tissue heterogeneity assessed with contrast-enhanced MRI predicts spontaneous ventricular arrhythmia in patients with ischemic cardiomyopathy and implantable cardioverter-defibrillator. *Circ Cardiovasc Imaging*. 2009;2:183–90.
94. Schelbert EB, Hsu LY, Anderson SA, Mohanty BD, Karim SM, Kellman P, et al. Late gadolinium-enhancement cardiac magnetic resonance identifies postinfarction myocardial fibrosis and the

- border zone at the near cellular level in ex vivo rat heart. *Circ Cardiovasc Imaging*. 2010;3(6):743–52.
95. Shambrook JS, Chowdhury R, Brown IW, Peebles CR, Harden SP. Cross-sectional imaging appearances of cardiac aneurysms. *Clin Radiol*. 2010;65(5):349–57.
 96. Kumar A, Abdel-Aty H, Kriedemann I, Schulz-Menger J, Gross CM, Dietz R, et al. Contrast-enhanced cardiovascular magnetic resonance imaging of right ventricular infarction. *J Am Coll Cardiol*. 2006;48(10):1969–76.
 97. Okayama S, Uemura S, Soeda T, Onoue K, Somekawa S, Ishigami KI, et al. Clinical significance of papillary muscle late enhancement detected via cardiac magnetic resonance imaging in patients with single old myocardial infarction. *Int J Cardiol*. 2011;146:73–9.
 98. Bogabathina H, Doyle M, Williams R, Yamrozik J, Vido D, Biederman RWW. Is there an alternative explanation to post-myocardial infarction emergence of mitral regurgitation? A CMR-LGE observational study. *J Heart Valve Dis*. 2013;22:669–74.
 99. Taylor AM, Dymarkowski S, Verbeken EK, Bogaert J. Detection of pericardial inflammation with late-enhancement cardiac magnetic resonance imaging: initial results. *Eur Radiol*. 2006;16(3):569–74.
 100. Bogaert J, Francone M. Cardiovascular magnetic resonance in pericardial diseases. *J Cardiovasc Magn Reson*. 2009;4:11.
 101. Srichai MB, Junor C, Rodriguez LL, Stillman AE, Grimm RA, Lieber ML, et al. Clinical, imaging, and pathological characteristics of left ventricular thrombus: a comparison of contrast-enhanced magnetic resonance imaging, transthoracic echocardiography, and transesophageal echocardiography with surgical or pathological validation. *Am Heart J*. 2006;152(1):75–84.
 102. Weinsaft JW, Kim HW, Shah DJ, Klem I, Crowley AL, Brosnan R, et al. Detection of left ventricular thrombus by delayed-enhancement cardiovascular magnetic resonance – prevalence and markers in patients with systolic dysfunction. *J Am Coll Cardiol*. 2008;52(2):148–57.
 103. Greaves SC, Zhi G, Lee RT, Solomon SD, MacFadyen J, Rapaport E, et al. Incidence and natural history of left ventricular thrombus following anterior wall acute myocardial infarction. *Am J Cardiol*. 1997;80(4):442–8.
 104. Chiarella F, Santoro E, Domenicucci S, Maggioni A, Vecchio C. Predischarge two-dimensional echocardiographic evaluation of left ventricular thrombosis after acute myocardial infarction in the GISSI-3 study. *Am J Cardiol*. 1998;81(7):822–7.
 105. Pfeffer MA, Braunwald E. Ventricular remodeling after myocardial-infarction – experimental-observations and clinical implications. *Circulation*. 1990;81(4):1161–72.
 106. Hutchins GM, Bulkley BH. Infarct expansion versus extension – 2 different complications of acute myocardial-infarction. *Am J Cardiol*. 1978;41(7):1127–32.
 107. Weisman HF, Bush DE, Mannisi JA, Weisfeldt ML, Healy B. Cellular mechanisms of myocardial infarct expansion. *Circulation*. 1988;78(1):186–201.
 108. Weber KT, Sun Y, Katwa LC. Wound healing following myocardial infarction. *Clin Cardiol*. 1996;19(6):447–55.
 109. Moss AJ. Risk stratification and survival after myocardial infarction. *N Engl J Med*. 1983;309(6):331–6.
 110. Larose E, Rodes-Cabau J, Pibarot P, Rinfret S, Proulx G, Nguyen CM, et al. Predicting late myocardial recovery and outcomes in the early hours of ST-segment elevation myocardial infarction: traditional measures compared with microvascular obstruction, salvaged myocardium, and necrosis characteristics by cardiovascular magnetic resonance. *J Am Coll Cardiol*. 2010;55(22):2459–69.
 111. Geskin G, Kramer CM, Rogers WJ, Theobald TM, Pakstis D, Hu Y-L, et al. Quantitative assessment of myocardial viability after infarction by dobutamine magnetic resonance tagging. *Circulation*. 1998;98:217–23.
 112. Klug G, Trieb T, Schocke M, Nocker M, Skalla E, Mayr A, et al. Quantification of regional functional improvement of infarcted myocardium after primary PTCA by contrast-enhanced magnetic resonance imaging. *J Magn Reson Imaging*. 2009;29(2):298–304.
 113. Rubenstein JC, Ortiz JT, Wu E, Kadish A, Passman R, Bonow RO, et al. Imaging and diagnostic testing – the use of periinfarct contrast-enhanced cardiac magnetic resonance imaging for the prediction of late postmyocardial infarction ventricular dysfunction. *Am Heart J*. 2008;156(3):498–505.
 114. Morishima I, Sone T, Okumura K, Tsuboi H, Kondo J, Mukawa H, et al. Angiographic no-reflow phenomenon as a predictor of adverse long-term outcome in patients treated with percutaneous transluminal coronary angioplasty for first acute myocardial infarction. *J Am Coll Cardiol*. 2000;36(4):1202–9.
 115. Symons R, Masci PG, Goetschalckx K, Doulatpatis K, Janssens S, Bogaert J. Effect of infarct severity on regional and global left ventricular remodeling in patients with successfully reperfused ST segment elevation myocardial infarction. *Radiology*. 2014;10:132746.
 116. Masci PG, Ganame J, Strata E, Desmet W, Aquaro GD, Dymarkowski S, et al. Myocardial salvage by CMR correlates with LV remodeling and early ST-segment resolution in acute myocardial infarction. *JACC Cardiovasc Imaging*. 2010;3(1):45–51.